LETTER

doi:10.1038/nature10599

Senescence surveillance of pre-malignant hepatocytes limits liver cancer development

Tae-Won Kang[1]*, Tetyana Yevsa[1,2]*, Norman Woller[2], Lisa Hoenicke[1], Torsten Wuestefeld[1,2], Daniel Dauch[1], Anja Hohmeyer[1,2], Marcus Gereke[1], Ramona Rudalska[1], Anna Potapova[1], Marcus Iken[3], Mihael Vucur[4], Siegfried Weiss[1], Mathias Heikenwalder[5,6], Sadaf Khan[7], Jesus Gil[7], Dunja Bruder[1], Michael Manns[2], Peter Schirmacher[8], Frank Tacke[4], Michael Ott[3], Tom Luedde[4], Thomas Longerich[8], Stefan Kubicka[9] & Lars Zender[1,2]

Upon the aberrant activation of oncogenes, normal cells can enter the cellular senescence program, a state of stable cell-cycle arrest, which represents an important barrier against tumour development *in vivo*[1]. Senescent cells communicate with their environment by secreting various cytokines and growth factors, and it was reported that this 'secretory phenotype' can have pro- as well as anti-tumorigenic effects[2–5]. Here we show that oncogene-induced senescence occurs in otherwise normal murine hepatocytes *in vivo*. Pre-malignant senescent hepatocytes secrete chemo- and cytokines and are subject to immune-mediated clearance (designated as 'senescence surveillance'), which depends on an intact CD4$^+$ T-cell-mediated adaptive immune response. Impaired immune surveillance of pre-malignant senescent hepatocytes results in the development of murine hepatocellular carcinomas (HCCs), thus showing that senescence surveillance is important for tumour suppression *in vivo*. In accordance with these observations, ras-specific Th1 lymphocytes could be detected in mice, in which oncogene-induced senescence had been triggered by hepatic expression of *Nras*^{G12V}. We also found that CD4$^+$ T cells require monocytes/macrophages to execute the clearance of senescent hepatocytes. Our study indicates that senescence surveillance represents an important extrinsic component of the senescence anti-tumour barrier, and illustrates how the cellular senescence program is involved in tumour immune surveillance by mounting specific immune responses against antigens expressed in pre-malignant senescent cells.

To investigate whether oncogene-induced senescence occurs in the mouse liver, we used hydrodynamic injection[6] to stably deliver transposable elements[7] expressing oncogenic *Nras* (*Nras*^{G12V}) into hepatocytes. Transposable elements encoding an effector loop mutant (*Nras*$^{G12V/D38A}$), incapable of signalling to downstream pathways[8], served as a control (Supplementary Fig. 1). Although Nras immunostainings revealed efficient transposon delivery in both groups (Fig. 1 and Supplementary Fig. 2), activated MAPK signalling (p-ERK immunostaining) could only be detected in animals transduced with *Nras*^{G12V} (Fig. 1). ERK phosphorylation was accompanied by a cellular senescence response as shown by stainings for p21, p16 and SA-β-gal (Fig. 1), and quantification of Nras-positive and p21- and p16-positive senescent cells revealed equal numbers, indicating that every *Nras*^{G12V}-expressing hepatocyte had entered the senescence program (Supplementary Fig. 3).

Microscopic examination of mouse livers harbouring pre-malignant senescent hepatocytes showed an inflammatory reaction with large clusters of immune cells surrounding morphologically altered, senescent hepatocytes (Fig. 2a). Similar findings were made when senescence was triggered by Cre-recombinase-mediated intrahepatic activation of an endogenous oncogenic *Kras* allele (*Kras*^{G12D})[9] (Supplementary Fig. 4).

To address whether the observed immune cell infiltration in oncogene-induced senescence mouse livers could be due to secreted cytokines, lysates from *Nras*^{G12V}- or *Nras*$^{G12V/D38A}$-transduced livers

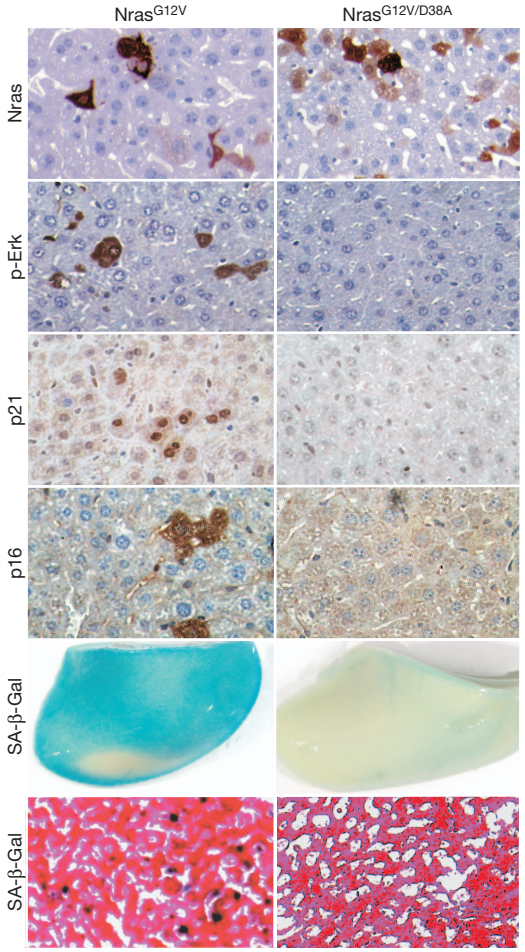

Figure 1 | Intrahepatic expression of oncogenic Nras^{G12V} induces cellular senescence. Stainings for Nras, p-Erk, p21, p16 and SA-β-Gal (×400) were performed on liver sections or resected liver lobes (SA-β-gal wholemount staining) 12 days after delivery of transposon constructs (see also Supplementary Fig. 1).

[1]Helmholtz Centre for Infection Research, Inhoffenstrasse 7, 38124 Braunschweig, Germany. [2]Hannover Medical School, Dept. of Gastroenterology, Hepatology and Endocrinology, Carl-Neuberg-Strasse 1, 30625 Hannover, Germany. [3]Twincore Centre for Experimental and Clinical Infection Research, Feodor-Lynen Strasse 7, 30625 Hannover, Germany. [4]Department of Internal Medicine III, University Hospital Aachen, 52074 Aachen, Germany. [5]Department of Pathology, University Hospital Zurich, CH 8091 Zurich, Switzerland. [6]Institute of Virology, Helmholtz Centre Munich, Technical University Munich, 81675 Munich, Germany. [7]MRC Clinical Sciences Centre, Faculty of Medicine, Imperial College, Hammersmith Campus, London W12 0NN, UK. [8]University of Heidelberg, Institute of Pathology, Im Neuenheimer Feld 220/21, 69120 Heidelberg, Germany. [9]Clinic for Internal Medicine, District Hospital Reutlingen, Steinenbergstrasse 31, 72764 Reutlingen, Germany.
*These authors contributed equally to this work.

©2011 Macmillan Publishers Limited. All rights reserved

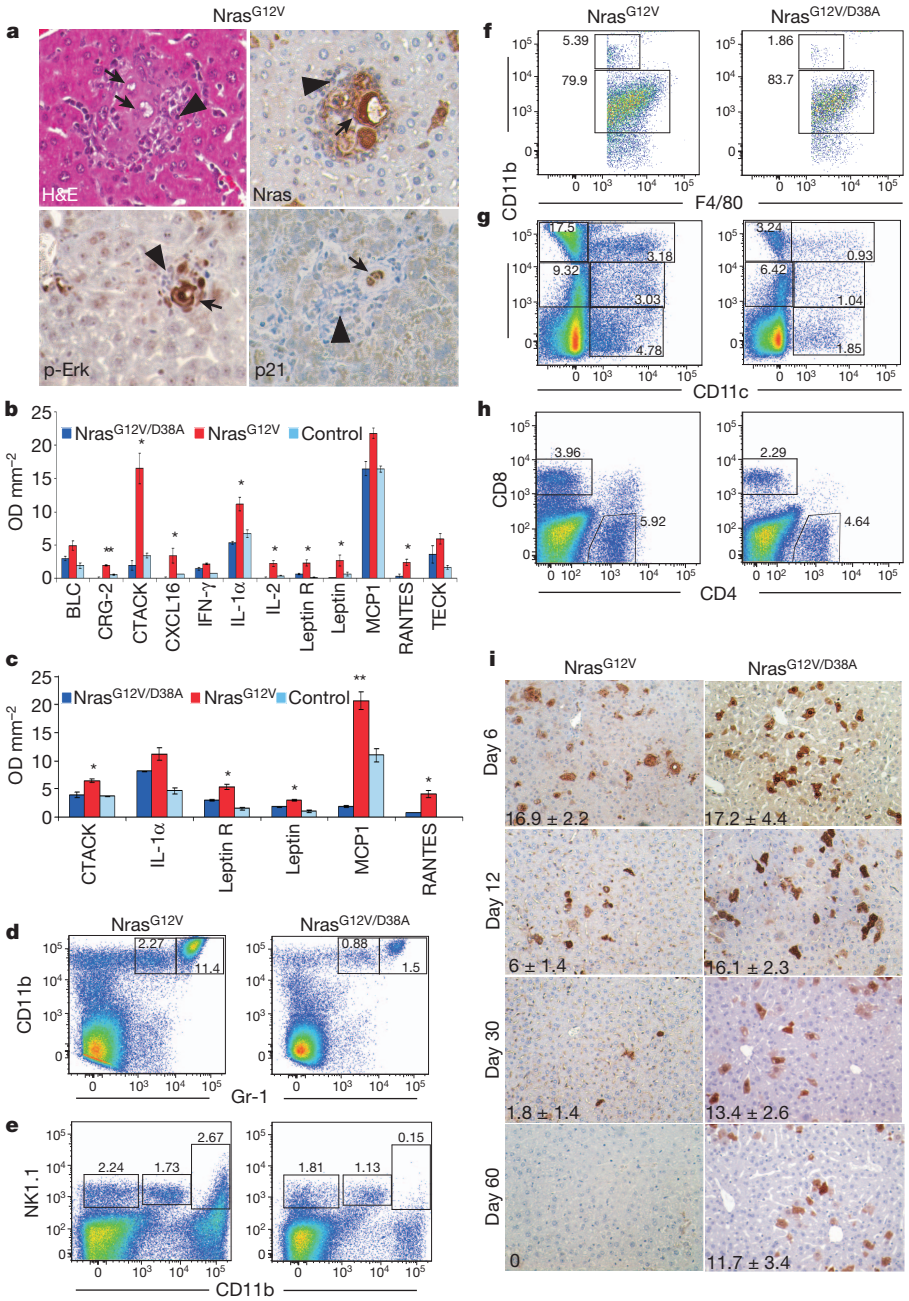

Figure 2 | Pre-malignant senescent hepatocytes are cleared by liver-infiltrating immune cells. **a**, Immune cell clusters were found in close proximity to pre-malignant senescent hepatocytes as shown by hematoxylin and eosin, Nras, p-Erk and p21 stainings (×400). Arrows, senescent hepatocytes; arrowheads, infiltrating immune cells. **b**, **c**, Oncogene-induced senescence in mouse hepatocytes leads to an increased expression of cyto-/chemokines as measured by cytokine arrays on whole liver lysates (**b**) or purified hepatocytes (**c**). OD, optical density. $^{**}P < 0.0048$ and $^{*}P < 0.0107$, each $Nras^{G12V}$ compared with $Nras^{G12V/D38A}$. **d–h**, Immunophenotyping and quantification of liver-infiltrating immune cells by flow cytometry: neutrophils/monocytes (**d**), NK cells (**e**), macrophages (**f**), dendritic cells (**g**) and $CD4^+$ and $CD8^+$ lymphocytes (**h**) (representative data from three independent experiments). **i**, Quantification of Nras-positive cells (×200) on liver sections collected from mice transduced with $Nras^{G12V}$ or $Nras^{G12V/D38A}$ at the indicated time points. Values represent mean ± s.d. ($n = 4$).

or purified hepatocytes thereof were analysed by cytokine arrays, which revealed that several cytokines were directly secreted by senescent hepatocytes (CTACK, interleukin-1α (IL-1α), leptin R, leptin, MCP1 and RANTES), whereas others seemed to be secreted by liver-infiltrating immune cells (CRG-2, interferon-γ (IFN-γ), IL-2, TECK) (Fig. 2b, c).

Using flow cytometry analyses on liver single-cell suspensions, we found that the inflammatory reaction in senescent mouse livers was composed of neutrophils ($CD11b^+/Gr\text{-}1^{high}$), monocytes ($CD11b^+/Gr\text{-}1^{int.}$) (Fig. 2d), natural killer (NK) cells ($NK1.1^+/CD11b^+$) (Fig. 2e), macrophages ($CD11b^{high}/F4/80^+$) (Fig. 2f) and $CD11c^+$ dendritic cells (Fig. 2g). Furthermore, an increased influx of $CD8^+$ as well as $CD4^+$ T cells was detected (Fig. 2h). An increased number of $CD4^+$ T lymphocytes and dendritic cells could also be detected in portal lymph nodes of mice injected with $Nras^{G12V}$ (Supplementary Fig. 5a, b). Immunohistochemical analyses confirmed that neutrophils, lymphocytes and monocytes/macrophages were found in immune cell clusters encircling hepatocytes expressing $Nras^{G12V}$ (Supplementary Fig. 6).

We next sought to investigate whether liver-infiltrating immune cells mediate the clearance of senescent hepatocytes. Although 6 days after *in vivo* delivery of $Nras^{G12V}$ or $Nras^{G12V/D38A}$ similar numbers of Nras-expressing cells were found in both groups, time-course analysis revealed a rapid loss of Nras-positive cells in $Nras^{G12V}$-transduced livers, with only 6 ± 1.4% of Nras-positive cells remaining at day 12 and no detectable Nras-positive cells after 60 days, whereas no such change was observed in $Nras^{G12V/D38A}$-transduced livers (Fig. 2i). Examination of livers by TdT-mediated dUTP nick end labelling (TUNEL) staining did not reveal significant differences, thus excluding the possibility that an increased cell death in $Nras^{G12V}$-transduced livers accounts for the decrease in Nras-positive cells (Supplementary Fig. 7).

To delineate which immune cells are mediating the clearance of senescent hepatocytes, we took advantage of syngeneic mice harbouring genetically defined immune defects: C.B-17 wild-type (WT) mice with an intact immunity, C.B-17 SCID mice harbouring an impaired adaptive immune response and C.B-17 SCID/beige mice, which furthermore exhibit defects in NK-cell and macrophage function

©2011 Macmillan Publishers Limited. All rights reserved

and generally in phagocytosis (Fig. 3a). Transposable elements encoding *Nras*^{G12V} or *Nras*$^{G12V/D38A}$ were intrahepatically delivered into these mice, and numbers of Nras-positive and senescent (p16- and p21-positive) hepatocytes were determined. As expected, C.B-17 WT mice showed an accented reduction of Nras-positive and senescent cells over time, with a complete loss of Nras-positive cells after 60 days (Fig. 3b–e). In strong contrast, no significant reduction in the number of Nras-positive cells was found in C.B-17 SCID mice after intrahepatic *Nras*^{G12V} delivery (Fig. 3b–e), thus suggesting that a defective adaptive immunity abrogates immune surveillance of pre-malignant senescent hepatocytes. Interestingly, significantly less p21- and p16 positive than Nras-positive hepatocytes could be detected at day 30 and 60 in C.B-17 SCID mice, suggesting that some Nras expressing hepatocytes at this time point have escaped the senescence program (Fig. 3b–e and Supplementary Fig. 8).

To explore the long-term consequences of defective senescence surveillance, we followed up C.B-17, C.B-17 SCID and C.B-17 SCID/beige mice after stable *in vivo* delivery of oncogenic *Nras*^{G12V} or *Nras*$^{G12V/D38A}$. We found dysplastic nodules, a bona fide precursor lesion for the development of HCC, as early as after 3 months

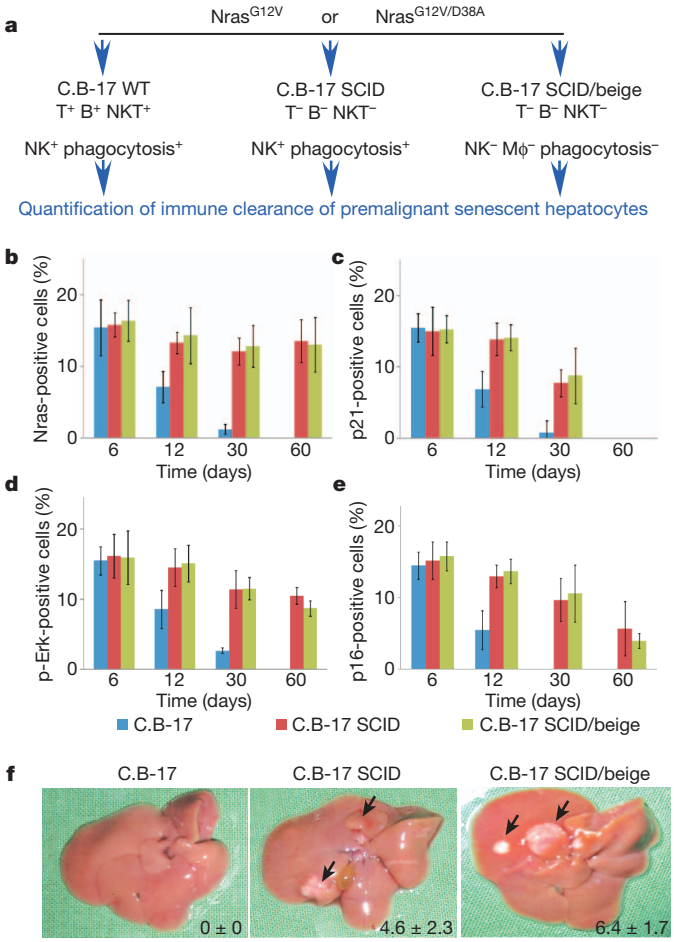

Figure 3 | Impaired senescence surveillance results in liver cancer development. **a**, Experimental setup and description of immune status of C.B-17 WT, C.B-17 SCID and C.B-17 SCID/beige mice. **b–e**, Quantification of Nras- (**b**), p21- (**c**), p-Erk- (**d**) and p16-positive cells (**e**) on liver sections from indicated mice after stable intrahepatic delivery of *Nras*^{G12V}. Values represent mean ± s.d. ($n = 4$). **f**, Impaired immune surveillance of pre-malignant senescent hepatocytes results in the development of HCC in C.B-17 SCID and C.B-17 SCID/beige mice that had been transduced with *Nras*^{G12V}. Shown are representative photographs of explanted livers ($n = 10$). Arrows, intrahepatic tumour nodules. Values represent mean ± s.d. of macroscopically detectable tumour nodules bigger than 3 mm in diameter.

(Supplementary Fig. 9a), followed by HCCs as early as 4 months, after intrahepatic delivery of oncogenic *Nras* in C.B-17 SCID and C.B-17 SCID/beige mice (Supplementary Fig. 9b and data not shown). Although after 7 months there was still no tumour growth in the control group (*Nras*$^{G12V/D38A}$-transduced mice) (Supplementary Fig. 10) and in Nras^{G12V}-expressing immunocompetent C.B-17 mice (Fig. 3f), severe intrahepatic tumour growth could be observed in *Nras*^{G12V}-transduced C.B-17 SCID as well as C.B-17 SCID/beige mice (Fig. 3f and Supplementary Fig. 11), suggesting that an impaired immune surveillance of pre-malignant senescent hepatocytes results in HCC development.

The SCID immune defect comprises defects in T lymphocyte, B lymphocyte and NKT cell function[10]. To address the role of these cell types in senescence surveillance, we next analysed senescence surveillance in Cd1d$^{-/-}$ (lacking NKT cells), CD8$^{-/-}$ and CD4$^{-/-}$ mice as well as in immunocompetent mice where CD4$^+$ and CD8$^+$ T cells had been depleted by antibodies. While Cd1d$^{-/-}$ and CD8$^{-/-}$ mice and those with antibody-mediated depletion of CD8$^+$ T cells displayed normal or nearly normal senescence surveillance (Supplementary Fig. 12 and Fig. 4a), a completely blunted senescence surveillance was observed in CD4$^{-/-}$ mice and mice of different H-2 haplotypes, in which CD4$^+$ T lymphocytes had been depleted by antibodies (Fig. 4a and Supplementary Fig. 13). CD4$^+$ T-cell-dependent surveillance of pre-malignant senescent hepatocytes was also found in a mouse model, wherein liver-specific activation of oncogenic ras was accomplished by a tamoxifen-inducible cre-recombinase[11,12] (Supplementary Fig. 14).

In line with these results, we observed that stable delivery of oncogenic *Nras*^{G12V} resulted in massive intrahepatic tumour growth in CD4$^{-/-}$ mice (Fig. 4b and Supplementary Fig. 15), whereas all arising tumours were found to harbour the Nras^{G12V} encoding transposon (Supplementary Fig. 16a, b). Western blotting of tumour protein lysates against p19^{Arf} suggested reduced p19^{Arf} expression as a potential mechanism that had allowed Nras^{G12V}-expressing hepatocytes to escape from the senescence arrest (Supplementary Fig. 17).

IFN-γ enzyme-linked immunospot (ELISPOT) assays with mutant Nras-specific 15-mer peptides revealed antigen-specific T cells in mice harbouring senescent hepatocytes (Nras^{G12V}) but not in mice expressing Nras$^{G12V/D38A}$ (Fig. 4c and Supplementary Fig. 18). To probe whether the induction of a mutant ras-specific immune response is indeed dependent on execution of the senescence program, we repeated our experiments in p19$^{Arf-/-}$ mice, in which the senescence program is genetically disabled[13]. Intrahepatic delivery of *Nras*^{G12V} into p19$^{Arf-/-}$ mice did not trigger ras-specific IFN-γ production (Fig. 4c, d); rather, it resulted in the rapid onset of invasive HCC, which was independent of the CD4$^+$ T-cell status (Supplementary Fig. 19a, b). Antigen-specific CD4$^+$ T-cell responses were confirmed in mice that had been transduced with transposons co-expressing *Nras*^{G12V} and haemagglutinin (HA), as ELISPOT assays with splenocytes of these mice indicated a strong, CD4$^+$ T-cell-specific immune response against HA (Supplementary Fig. 20a). No significant IL-4 and IL-17 responses could be measured in these experiments, thus suggesting that the observed response represents a Th1-polarized CD4$^+$ T-cell response (Supplementary Fig. 20a–c).

We next sought to explore whether senescence surveillance also occurs in inflammation-based HCC mouse models. For this, we analysed CD4$^+$ T-cell-dependent senescence surveillance and tumour development in mice with liver-specific ablation of MAP3-kinase transforming growth factor (TGF)-β-activated kinase 1 (Tak1)[14]. Antibody-mediated depletion of CD4$^+$ T cells resulted in a strong accumulation of senescent hepatocytes in Tak1$^{-/-}$ mice, which correlated with increased liver tumour development already at 3 months of age (Supplementary Fig. 21a–c). Furthermore, we quantified senescent hepatocytes in livers of Rag1$^{-/-}$ or syngeneic WT mice, which had been subjected to the diethylnitrosamine (DEN) liver carcinogen[15]. Interestingly, Rag1$^{-/-}$ mice showed an accumulation

©2011 Macmillan Publishers Limited. All rights reserved

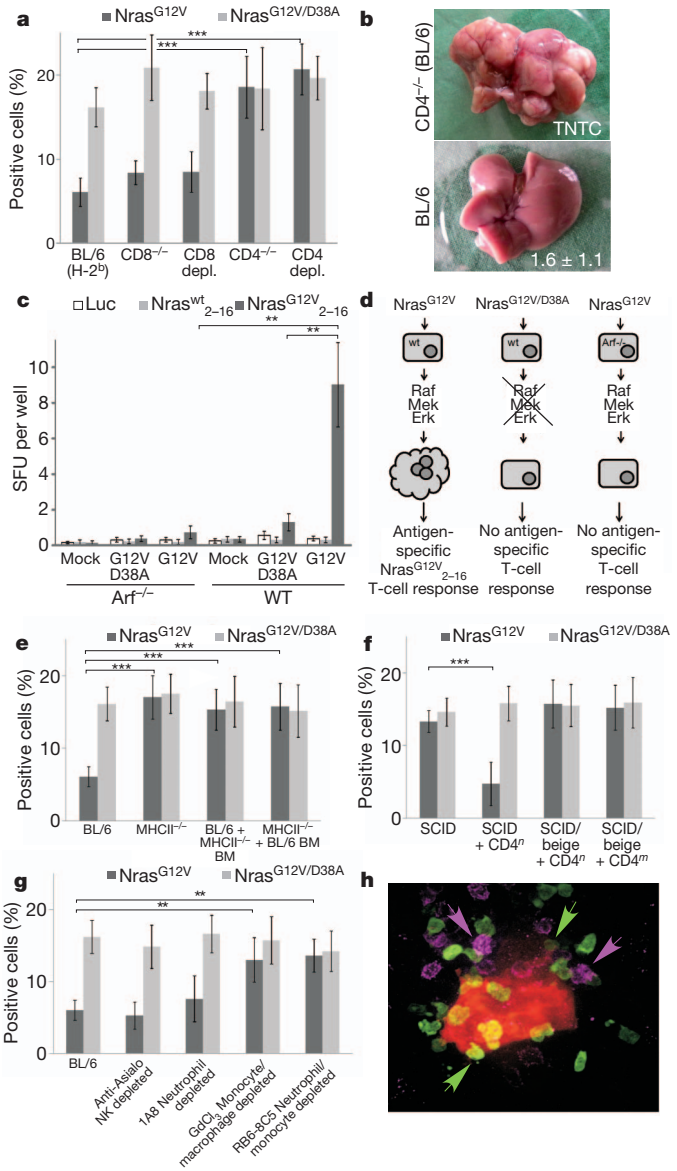

Figure 4 | Immune surveillance of pre-malignant senescent hepatocytes is orchestrated by antigen-specific CD4$^+$ T cells. **a**, Quantification of Nras-positive cells on liver sections from WT (C57BL/6), CD4$^{-/-}$, CD8$^{-/-}$ mice or CD4- or CD8-depleted WT mice 12 days after intrahepatic delivery of *Nras*^{G12V} or *Nras*$^{G12V/D38A}$ ($n = 5$). Values represent mean ± s.d. ***$P < 0.0004$ (*Nras*^{G12V}, C57BL/6 compared with CD4$^{-/-}$), ***$P < 0.0001$ (*Nras*^{G12V}, C57BL/6 compared with CD4 depleted). **b**, Impaired senescence surveillance results in the development of HCCs in CD4$^{-/-}$ mice 7 months after intrahepatic delivery of *Nras*^{G12V} ($n = 10$). Values represent mean ± s.d. of macroscopically detectable tumour nodules bigger than 3 mm in diameter (TNTC, too numerous to count). **c**, IFN-γ ELISPOT assay performed on splenocytes isolated from WT or p19$^{Arf-/-}$ mice 20 days after intrahepatic delivery of *Nras*^{G12V} or *Nras*$^{G12V/D38A}$. Results are represented as spot-forming units (SFU) per well ± s.e.m. ($n = 8$; **$P < 0.0026$ (Nras$^{G12V}{}_{2\text{-}16}$, C57BL/6/ Nras^{G12V} compared with p19$^{Arf-/-}$/Nras^{G12V}), **$P < 0.0065$ (Nras$^{G12V}{}_{2\text{-}16}$, C57BL/6/ Nras^{G12V} compared with C57BL/6 Nras$^{G12V/D38A}$)). **d**, Representation of the pathway: induction of an antigen-specific immune response is dependent on the execution of the senescence program. **e**, Quantification of Nras-positive cells 12 days after intrahepatic delivery of *Nras*^{G12V} or *Nras*$^{G12V/D38A}$ on liver sections from C57BL/6 WT, MHCII$^{-/-}$ mice and chimaeras as described in Supplementary Fig. 23a–d ($n = 5$; ***$P < 0.0003$). **f**, Quantification of Nras-positive cells on liver sections from C.B-17 SCID mice, C.B-17 SCID mice adoptively transferred with syngeneic CD4$^+$ T cells, and C.B-17 SCID/beige mice adoptively transferred with syngeneic CD4$^+$ T cells (CD4^n, naive; CD4^m, memory) 12 days after intrahepatic delivery of *Nras*^{G12V} or *Nras*$^{G12V/D38A}$ ($n = 5$; ***$P < 0.0002$). **g**, Quantification of Nras-positive cells on liver sections from untreated, NK cell-depleted, Ly-6G-depleted (clone 1A8), $GdCl_3$-depleted and Ly-6G/Ly-6C (clone RB6-8C5)-depleted C57BL/6 mice 12 days after intrahepatic delivery of *Nras*^{G12V} or *Nras*$^{G12V/D38A}$ ($n = 5$). Values represent mean ± s.d. (**$P < 0.0054$). **h**, Confocal microscopy on lys-EGFP transgenic mouse livers (EGFP$^+$ monocytes/macrophages and neutrophils). Senescent hepatocytes stain orange (co-expression of oncogenic Nras^{G12V} with TagRFP). Green arrows, EGFP-positive monocytes/macrophages and neutrophils; pink arrows, APC-labelled lymphocytes (×600).

of senescent hepatocytes 24 weeks after DEN administration (Supplementary Fig. 22a, b), which was associated with an accelerated and increased tumorigenesis at later time points (data not shown, and F. Tacke and C. Schneider, unpublished observations). As the *Rag1*$^{-/-}$ gene defect comprises both CD4 and CD8 deficiency, further work is needed to delineate the role of CD4$^+$ and CD8$^+$ T cells in this model.

It has been described that hepatocytes can directly present antigens through major histocompatibility complex class II (MHCII); however, the significance of this process is still under debate. We studied antigen-specific CD4$^+$ T-cell activation in mice with liver- or bone-marrow-specific MHCII deficiency and found that CD4$^+$ T-cell activation depends on the presence of professional antigen presenting cells (APCs) (Supplementary Fig. 23 and supplementary data description). These findings were corroborated by *in vitro* co-incubation assays of senescent, Nras^{G12V}-HA-expressing hepatocytes with TCR-HA CD4$^+$ T cells, confirming that proliferation was dependent on the presence of MHCII-matched APCs and cytokine secretion from senescent hepatocytes and immune cells (Supplementary Fig. 24a, b). Furthermore, functional *in vivo* experiments revealed a crucial role for M1 cytokines, in particular IL-1α, in senescence surveillance (Supplementary Fig. 25), whereas cytokine secretion seems to be p38 MAPK dependent (Supplementary Fig. 26a, b).

Interestingly, we could detect upregulation of MHCII on a subfraction of senescent hepatocytes and concomitant upregulation of co-stimulatory CD86 on some cells (Supplementary Fig. 24c). It is noteworthy that, although not sufficient to induce proliferation of naive CD4$^+$ T cells, hepatic MHCII expression appears to be necessary to allow a directed killing of pre-malignant senescent hepatocytes as senescence surveillance was significantly impaired in mice with liver-specific MHCII deficiency (Fig. 4e).

Finally, we addressed whether senescent hepatocytes are directly killed by cytotoxic CD4$^+$ T cells[16] or whether CD4$^+$ T cells require innate immune cells to execute the killing. We found that adoptive transfer of syngeneic CD4$^+$ T cells into *Nras*^{G12V}-injected C.B-17 SCID mice restored senescence surveillance (Fig. 4f) and suppressed tumour development in these mice (Supplementary Fig. 27). However, even the adoptive transfer of 'memory' CD4$^+$ T cells (obtained from immunocompetent C.B-17 mice with hepatic Nras^{G12V} expression) did not restore senescence surveillance in C.B-17 SCID/beige mice (Fig. 4f), suggesting that CD4$^+$ T cells act in a T-helper cell manner and require innate immune cells to kill pre-malignant senescent cells. In accordance with these results, we found that gadolinium treatment of mice, which depletes macrophages and affects monocytes[17], dramatically reduced senescence surveillance (Fig. 4g). In contrast, selective depletion of neutrophils (Ly-6G antibody) only marginally affected senescence surveillance, and antibody-mediated depletion of NK cells showed no effect at all (Fig. 4g). To distinguish whether Kupffer cells as resident liver macrophages execute the killing for CD4$^+$ T cells or whether freshly infiltrated monocytes and replenished macrophages thereof are needed, we took advantage of the RB6-8C5 (Ly-6G/Ly-6C) antibody, which depletes neutrophils and monocytes, but does not affect tissue-resident macrophages[18]. Interestingly, monocyte depletion by RB6-8C5 completely abrogated senescence surveillance (Fig. 4g), thus pinpointing monocytes and probably freshly replenished macrophages thereof as effector cells. The interaction between CD4$^+$ T cells and monocytes/macrophages was

©2011 Macmillan Publishers Limited. All rights reserved

confirmed by confocal microscopy on Lys-enhanced green fluorescent protein (EGFP) transgenic mouse livers, where Lys-EGFP-positive cells ($EGFP^+$ macrophages, monocytes and neutrophils) and APC-labelled lymphocytes were found in close proximity to senescent $Nras^{G12V}$/TaqRFP-co-expressing hepatocytes (Fig. 4h).

Finally, to explore whether senescence surveillance occurs in human livers, we quantified senescent cells in patients infected with hepatitis C virus (HCV) with or without concomitant human immunodeficiency virus (HIV) infection (impaired $CD4^+$ T-cell function) and found that senescent (p16-positive) cells significantly accumulated in livers of patients with HIV (Supplementary Fig. 28a, b). Furthermore, we analysed a unique cohort of patients who underwent two subsequent liver transplantations due to HCV-induced liver cirrhosis with a comparable grade of liver damage. We quantified senescent cells in the patients' own explant livers (no immunosuppressive therapy, 'HCV-Tx') and in the explanted transplant liver after the development of re-cirrhosis (patient has been under immunosuppressive therapy, 'HCV-Re-Tx') and found that senescent hepatocytes significantly accumulate in livers under immunosuppressive therapy (Supplementary Fig. 28a, b), thus providing the first evidence for immune surveillance of senescent hepatocytes in human livers and one possible explanation for the increased rates of hepatocellular carcinoma found in HIV-infected patients or those under immunosuppressive therapy (reviewed in ref. 19).

Taken together, our results establish senescence surveillance as an important extrinsic component of the senescence anti-tumour barrier. Our data suggest that pre-malignant hepatocytes can escape the senescence arrest and contribute to development of liver cancer, thus emphasizing the importance of senescence surveillance. Our results on senescence escape of pre-malignant hepatocytes are in line with published reports demonstrating that senescence escape can occur *in vitro*[20,21], although it is formally possible that escaping cells initiate the senescence program (and thus display senescence markers) but never achieve the final state. Furthermore, it will be important to characterize whether factors secreted from pre-malignant senescent hepatocytes also contribute to the oncogenic transformation of neighbouring cells.

Recent work has shown that innate immune cells alone are sufficient to mediate the clearance of ras-driven liver carcinomas, wherein senescence was triggered by reactivation of endogenous p53[3]. In contrast, here we show that senescence surveillance of pre-malignant hepatocytes is orchestrated by antigen-specific $CD4^+$ T cells.

We anticipate that strategies specifically harnessing the identified mechanism of senescence surveillance hold great promise for improving cancer prevention and therapy. Furthermore, use of the senescence program to trigger or enhance antigen-specific immune responses will very probably find broad applications to improve vaccination strategies.

METHODS SUMMARY

For transposon-mediated intrahepatic gene transfer mice received a 5:1 molar ratio of transposon- to transposase encoding vector (30 μg total DNA). DNA was suspended in saline solution at a final volume of 10% of the animals' body weight and administered by hydrodynamic tail vein injection. Immunohistochemical analyses were performed on paraffin-embedded liver sections (citrate buffer antigen retrieval) using the indicated antibodies with standard protocols.

Received 14 July 2010; accepted 30 September 2011.
Published online 9 November 2011.

1. Narita, M. & Lowe, S. W. Senescence comes of age. *Nature Med.* **11,** 920–922 (2005).
2. Krtolica, A., Parrinello, S., Lockett, S., Desprez, P. Y. & Campisi, J. Senescent fibroblasts promote epithelial cell growth and tumorigenesis: a link between cancer and aging. *Proc. Natl Acad. Sci. USA* **98,** 12072–12077 (2001).
3. Xue, W. *et al.* Senescence and tumour clearance is triggered by p53 restoration in murine liver carcinomas. *Nature* **455,** 656–660 (2007).
4. Acosta, J. C. *et al.* Chemokine signaling via the CXCR2 receptor reinforces senescence. *Cell* **133,** 1006–1018 (2008).
5. Kuilman, T. *et al.* Oncogene-induced senescence relayed by an interleukin-dependent inflammatory network. *Cell* **133,** 1019–1031 (2008).
6. Hickman, M. A. *et al.* Gene expression following direct injection of DNA into liver. *Hum. Gene Ther.* **5,** 1477–1483 (1994).
7. Carlson, C. M., Frandsen, J. L., Kirchhof, N., McIvor, R. S. & Largaespada, D. A. Somatic integration of an oncogene-harboring Sleeping Beauty transposon models liver tumor development in the mouse. *Proc. Natl Acad. Sci. USA* **102,** 17059–17064 (2005).
8. Khwaja, A., Rodriguez-Viciana, P., Wennstrom, S., Warne, P. H. & Downward, J. Matrix adhesion and Ras transformation both activate a phosphoinositide 3-OH kinase and protein kinase B/Akt cellular survival pathway. *EMBO J.* **16,** 2783–2793 (1997).
9. Jackson, E. L. *et al.* Analysis of lung tumor initiation and progression using conditional expression of oncogenic K-ras. *Genes Dev.* **15,** 3243–3248 (2001).
10. Thomsen, M., Galvani, S., Canivet, C., Kamar, N. & Bohler, T. Reconstitution of immunodeficient SCID/beige mice with human cells: applications in preclinical studies. *Toxicology* **246,** 18–23 (2008).
11. Tannour-Louet, M., Porteu, A., Vaulont, S., Kahn, A. & Vasseur-Cognet, M. A tamoxifen-inducible chimeric Cre recombinase specifically effective in the fetal and adult mouse liver. *Hepatology* **35,** 1072–1081 (2002).
12. Harada, N. *et al.* Hepatocarcinogenesis in mice with β-catenin and Ha-ras gene mutations. *Cancer Res.* **64,** 48–54 (2004).
13. Kamijo, T. *et al.* Tumor suppression at the mouse INK4a locus mediated by the alternative reading frame product p19ARF. *Cell* **91,** 649–659 (1997).
14. Bettermann, K. *et al.* TAK1 suppresses a NEMO-dependent but NF-κB-independent pathway to liver cancer. *Cancer Cell* **17,** 481–496 (2010).
15. Sarma, D. S., Rao, P. M. & Rajalakshmi, S. Liver tumour promotion by chemicals: models and mechanisms. *Cancer Surv.* **5,** 781–798 (1986).
16. Brown, D. M. Cytolytic CD4 cells: direct mediators in infectious disease and malignancy. *Cell. Immunol.* **262,** 89–95 (2010).
17. Frid, M. G. *et al.* Hypoxia-induced pulmonary vascular remodeling requires recruitment of circulating mesenchymal precursors of a monocyte/macrophage lineage. *Am. J. Pathol.* **168,** 659–669 (2006).
18. Silva, M. T. When two is better than one: macrophages and neutrophils work in concert in innate immunity as complementary and cooperative partners of a myeloid phagocyte system. *J. Leukoc. Biol.* **87,** 93–106 (2010).
19. Hensel, M. *et al.* HIV and cancer in Germany. *Dtsch. Arztebl. Int.* **108,** 117–122 (2011).
20. Sage, J., Miller, A. L., Perez-Mancera, P. A., Wysocki, J. M. & Jacks, T. Acute mutation of retinoblastoma gene function is sufficient for cell cycle re-entry. *Nature* **424,** 223–228 (2003).
21. Dirac, A. M. & Bernards, R. Reversal of senescence in mouse fibroblasts through lentiviral suppression of p53. *J. Biol. Chem.* **278,** 11731–11734 (2003).

Supplementary Information is linked to the online version of the paper at www.nature.com/nature.

Acknowledgements We thank D. Largaespada and M. Kay for providing transposon vectors and transposase encoding vectors. We thank L. Gröbe, A. Rinkel, N. Struever, H. Riedesel, the team of the Helmholtz Centre for Infection Research (HZI) animal facility, M. Rothe, K. Schulze, A. Kobold, F. Heinzmann, N. Jedicke, C. Schneider, M. Pesic, H. Klimek and A. Samuels for technical assistance and assistance with animal work, and F. Alves, S. Kimmina, C. Dullin and S. Greco for assistance with flat panel-volumetric computer tomography. We thank the tissue bank of the National Center for Tumor Diseases Heidelberg for providing liver explant tissues. We thank S. Lowe, H. Tillmann, F. Greten and members of the Lowe and Zender laboratory for advice and discussions. This work was supported by the Helmholtz Association of German Research Centres (VH-NG-424 to L.Z.), the German Research Foundation, DFG (Emmy Noether Programme ZE 545/2-1 to L.Z., SFB/TRR77 and the 'Rebirth' Cluster of Excellence), the Wilhelm Sander Stiftung, the Bear Necessities Pediatric Cancer Foundation, the Federal German Ministry for Education and Research (BMBF) (ARCHES AWARD to L.Z.) and the European Commission (project 'Heptromic'). L.Z. holds an adjunct assistant Professorship with the Cold Spring Harbor Laboratory, Cold Spring Harbor, New York, USA. This work is dedicated to J. Wehland.

Author Contributions L.Z. designed and guided the research and wrote the manuscript. T.-W.K., T.Y. and N.W. conducted experiments and contributed to research design and manuscript preparation. L.H., T.W., D.D., A.H., M.G., R.R., A.P., M.I., M.V., S.W., M.H., S.K., J.G., F.T., To.L., D.B. M.M., M.O. and S.K. contributed to research design and/or conducted experiments. P.S. and Th.L. performed histopathological analyses.

Author Information Reprints and permissions information is available at www.nature.com/reprints. The authors declare no competing financial interests. Readers are welcome to comment on the online version of this article at www.nature.com/nature. Correspondence and requests for materials should be addressed to L.Z. (Lars.Zender@helmholtz-hzi.de).

©2011 Macmillan Publishers Limited. All rights reserved